IEEE Access
Multidisciplinary ⋮ Rapid Review ⋮ Open Access Journal

Received December 11, 2017, accepted January 21, 2018, date of publication February 2, 2018, date of current version April 18, 2018.

Digital Object Identifier 10.1109/ACCESS.2018.2801458

A Novel Constant Output Powers Compound Control Strategy for Variable-Speed Variable-Pitch Wind Turbines

HAIJUN REN, HAO ZHANG, HUANHUI ZHOU, PING ZHANG, XIN LEI, GUANG DENG, AND BIN HOU
School of Advanced Manufacture and Engineering, Chongqing University of Posts and Telecommunications, Chongqing 400065, China
Corresponding author: Haijun Ren (renhj@cqupt.edu.cn).

This work was supported by the National Natural Science Fund of China under Grant 51405052.

ABSTRACT The output power of wind turbine should be maintained at rated value when wind speed exceeds rated speed.However, the wind turbine is a system with large nonlinearity and time delay. Therefore, it is difficult for conventional linear controllers to realize effective control. In order to solve this problem, a combination of feedforward control with feedback control is developed. In feedback loop, feedback linearization theory is adopted to overcome the nonlinear features, and sliding mode algorithm is employed to improve the robustness of the system. On the other hand, in feedforward loop, a cerebellar model articulation controller is implemented to approximate the system. Furthermore, an improved credit assignment method is used to adjust the weight of the network. Together these procedures improve the effectiveness of the algorithm. Through this method, not only can the stability of the nonlinear model be ensured, but also the control lag caused by the time-delayed system can be compensated. Simulation results show that the feedforward-feedback compound control algorithm can both keep the output power at rated value and improve dynamic response speed, reduce adjustment time, has small steady-state error.

INDEX TERMS Feedback linearization, sliding mode control, ICA-CMAC, wind energy, pitch control.

I. INTRODUCTION

In order to reduce both environmental pollution and chemical energy consumption, wind energy is being widely developed by a growing number of countries [1]–[9]. However, wind turbines operate in a highly complex working environment, which is affected by a variety of factors. Varying wind speed has a great influence on the performance of a wind turbine. When the wind speed exceeds the rated value, the output power of the wind turbine must be maintained at the rated value. If one only relies on the blade's aerodynamics to regulate the output power, the output value becomes uncontrollable. Consequently, the power generation quality and the reliability of the wind turbine are both degraded. In order to address these problems, pitch control technologies have been largely adopted [10]–[15]. Recently, the large scale variable-speed variable-pitch wind turbine has become the mainstay of steam production worldwide. When the wind speed exceeds the rated value, the angle of the blade is adjusted to keep the output power constant. Many control strategies and algorithms are used in pitch systems to improve the control performance [16]–[26]. Civelek *et al.* [18] proposed a new intelligent genetic algorithm (IGA) to adjust the parameters of conventional PID. Compared with conventional genetic algorithm, the IGA adopted a new method, in which both the crossover point value and mutation rate were increased to enhance the iteration limit number so that the optimized parameters could be obtained. Simulation results showed that the system efficiency using the IGA was about 17% greater than that of the system adjusted by the GA. Zhu *et al.* [19] adopted a method known as H_2/H_∞-based pitch control. Due to the strongly nonlinear character and sensitivity to external disturbance of wind turbines, controller design is a focus. In order to reduce the pitch angle error, Corradini *et al.* [20] designed an observer-based controller, in which wind speed was assumed rather than measured. Furthermore, a sliding surface was defined. Then, the stability of the proposed controller was proven by theoretical calculation and the proposed method was verified by using FAST software. Basing on FAST, Lasheen and Elshafei [21] designed a fuzzy-model predictive controller to adjust the pitch angle.

Although nonlinear models with higher accuracy, the authors used a linear model in the fuzzy system. However, a nonlinear model would increase computational difficulty. In their paper, the proposed controller could address nonlinear problem. Furthermore, a Kalman observer was adopted to estimate immeasurable system states. Thus the system performance was further improved. Yilmaz and Özer [22] employed two neuro-controllers to adjust pitch angle to obtain the most suitable output power when the wind speed exceeds the rated value. In their paper, the proposed MLP-NNC-based controller could closely approximate the nonlinearity of the wind turbine. However, other studies have shown that the performance of RBF-based controllers is better than that of MLP-NNC-based controllers. Xiao *et al.* [23] proposed a fuzzy algorithm to maintain the output power at the rated value, which has the advantage of approximating the nonlinear system without an accurate mathematical model. The unwanted absorptions of output power were greatly reduced based on the fuzzy rules designed by the algorithm. Bagheri and Sun [24] proposed a Nussbaum-type function and an adaptive radial-basis function neural network to address the nonlinear problem of a wind turbine. Furthermore, the Lyapunov stability of the system was analyzed.

In this paper, a novel compound control algorithm is proposed to enhance controller performance and maintain output power at rated value when wind speed exceeds its rated speed. As wind turbine is a strongly nonlinear system, in [27], conventional linear PID controller was adopted as a feedback controller and it is not meet control requirements. In order to overcome nonlinear problem, several control algorithms are proposed in [28]–[33]. Feedback linearization theory is a classic approch addressing nonlinear problem [28]. As the effects of parameters varying and external disturbances, however, the robustness of feedback linearization controller should be improved. Sliding mode algorithm can address the problems of parameters varying and external disturbances [34]–[41]. Thus, in feedback loop, we adopt sliding mode algorithm to enhance the robustness of feedback linearization so that system tracking control performance is also improved. And wind turbine is a time delay system, reseachers adopted many advanced control approaches to overcome time delay problem [42], [43]. However, only is feedback controller hard to effectively address the problem. Thereby, feedforward controller is proposed to compensate time delay. In [27], CMAC network was adopted as feedforward controller, in which errors are evenly distributed to each activated unit. Thus, learning rate of the CMAC network is slow. In order to improve learning rate, we propose an improved credit assignment approch (ICA) to optimize CMAC. The main contributions of this paper are threefold: (i) To improve tracking control performance as well as to attenuate the effects of time delay and uncertain distuebances, a feedforward-feedback compound control constructure is presented; (ii) At initial time, neural network needs to learn feedback control algorithm, in which feedback control performance will affect the neural network performance. Thus, sliding mode theory is adopted to optimize feedback linearization algorithm as well as two disturbance variables are considered in wind turbine model. Further, system Lyapunov stability is proven; (iii) Since learning rate is slow in CMAC network, an improved credit assignment (ICA) approach is adopted optimize network weight, in which lower credit weights are adjusted more than higher credit weights. And then the network performance is improved.

II. MODELING FOR WIND TURBINE SYSTEM

A wind turbine is a device that converts wind energy into electrical energy, with a shaft power that can be expressed by [23, eq. (1)].

$$P = \frac{1}{2}\rho\pi R^2 v^3 C_p(\lambda, \beta) \tag{1}$$

where P is the shaft power of the wind turbine, ρ is the air density, R is the radius of the wind wheel, v is the wind speed, $C_p(\lambda, \beta)$ is the rotor power coefficient, λ is the tip speed ratio, and β is the pitch angle.

From Equation (1), the shaft power of the wind turbine is determined by the wind speed and rotor power coefficient when the radius of the rotor has been selected. The rotor power coefficient is expressed as follows[23].

$$\begin{aligned} C_p(\lambda, \beta) = (0.44 - 0.0167\beta)\sin(\frac{\pi(\lambda-3)}{15-0.3\beta}) \\ - 0.00184(\lambda - 3)\beta \end{aligned} \tag{2}$$

Here

$$\lambda = \frac{\omega_r R}{v} \tag{3}$$

where ω_r is the rotor speed.

Drive train of stiffness model is adopted [19]. Therefore, the relationship between low-speed shaft and high-speed shaft is expressed as follows [44].

$$\dot{\omega_r}(J_r + k^2 J_g) = T_r - kT_e \tag{4}$$

where J_r is the inertia moment of the wind wheel, k is the drive ratio, J_g is the inertia moment of the generator, T_r is the aerodynamical torque of the wind wheel, and T_e is the electromagnetic torque.

As the electro-hydraulic proportional valves work stably and have a long life, it is widely used in wind turbine systems [45], [46]. In this paper, the transfer function model of the hydraulic pitch system can be expressed by Equation (5).

$$G(s) = \frac{Y(s)}{I(s)} = \frac{K_d}{s(\frac{s^2}{\omega_h^2} + \frac{2\varepsilon_h}{\omega_h} + 1) + K_d K_s} \tag{5}$$

where $G(s)$ is the system transfer function, $Y(s)$ is the output transfer function, $I(s)$ is the input transfer function, K_d is the proportional coefficient of the electrohydraulic system, ε_h is the damping ratio of the hydraulic mechanism, ω_h is the natural frequency of the hydraulic system, and K_s is the feedback coefficient.

Since the natural frequency of the pitch system is much larger than that of the wind turbine, the variable-pitch hydraulic system can be used as the first-order system as follows.

$$G(s) = \frac{Y(s)}{I(s)} = \frac{K_d}{s + K_d K_s} \quad (6)$$

According to double-fed generator equivalent circuit, stator equation and rotor equation, the expression of the electromagnetic torque can be expressed by Equation (7).

$$\begin{aligned} T_{em} &= \frac{-3spx_m^2 r_2}{\omega_1 c^2} U_1^2 + \frac{3px_m^2 r_1}{\omega_1 c^2} U_2^2 \\ &+ \frac{3px_m}{\omega_1 c^2}[(r_1 r_2 + sx_{2\sigma}x_{1\sigma} + sx_m^2)\sin\alpha_{12} \\ &- (sx_{2\sigma}r_1 - x_{1\sigma}r_2)\cos\alpha_{12}]U_1 U_2 \end{aligned} \quad (7)$$

where $c = \sqrt{(r_1 r_2 - sx_{2\sigma}x_{1\sigma} + sx_m^2)^2 + (sx_{2\sigma}r_1 + x_{1\sigma}r_2)^2}$, p is the pole pairs, ω_1 is the synchronous angular velocity, s is the slip rate, U_1 is the stator voltage, U_2 is the rotor voltage, α_{12} is the phase difference between stator and rotor, r_1 is the stator winding resistance, $x_{1\sigma}$ is the leakage reactance, r_2 is the rotor winding resistance calculated to stator, $x_{2\sigma}$ is the leakage calculated to stator side, x_m is the excitation reactance.

Electromagnetic power of doubly-fed generator can be expressed by Equation(8).

$$\begin{aligned} P_e &= T_{em}\Omega_1 = T_{em}\frac{\omega_1}{p} = \frac{-3sx_m^2 r_2}{c^2}U_1^2 + \frac{3x_m^2 r_1}{c^2}U_2^2 \\ &+ \frac{3x_m}{c^2}[(r_1 r_2 + sx_{2\sigma}x_{1\sigma} + sx_m^2)\sin\alpha_{12} \\ &- (sx_{2\sigma}r_1 - x_{1\sigma}r_2)\cos\alpha_{12}]U_1 U_2 \end{aligned} \quad (8)$$

where Ω_1 is the generator synchronous mechanical angular velocity.

III. COMPOUND CONTROL BASED ON FEEDBACK LINEARIZATION WITH SLIDING MODE AND ICA-CMAC

In order to control the wind turbine, which is a strongly nonlinear system with large hysteresis, the feedforward-feedback compound control strategy is adopted. In feedback control loop, feedback linearization theory is proposed. Nevertheless, there are uncertain disturbances in wind farm and construction parameters varying so that the model of wind turbine is unprecise. Thus, the robustness of the system adopting feedback linearization theory should be enhanced. In order to address this problem, sliding mode algorithm is employed to improve the robustness of the system. On the other hand, CMAC algorithm is implemented in the feedforward control loop. Conventionally, in CMAC network, the error is assumed to be equally distributed among all the activated memory cells, rather than considering the individual contribution of each cell to the error, and the weights that are adjusted at different times are assumed to have the same credit. Therefore, the real-time performance of the network is reduced. In this paper, the weights of high credit are not adjusted while the weights of low credit are adjusted. At the same time, a balance learning process is developed to further optimize the method for adjusting the weights. Thus, the learning efficiency of the network is improved. The compound control strategy is shown in Figure 1.

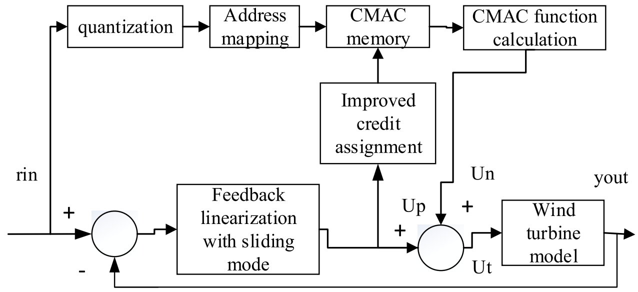

FIGURE 1. Block diagram of compound control strategy for wind turbines.

A. FEEDBACK LINEARIZATION WITH SLIDING MODE CONTROL FOR WIND TURBINE

The differential equations of the wind turbine can be obtained from Section II. Furthermore, for model uncertainty, some factors should be considered [47]. To verify the system robustness, some researchers even considered the situation of sensor failure [48], [49]. In the paper, two uncertain variables are included in the models of wind turbine.

$$\begin{cases} \dot{\omega_r}(J_r + k^2 J_g) = \frac{1}{2\omega_r}\rho\pi R^2 v^3 C_p(\lambda,\beta) - kT_{em} + d_1 \\ \dot{\beta} = K_d K_s(\frac{1}{K_s}\beta_1 - \beta) + d_2 \end{cases} \quad (9)$$

where d_1 and d_2 are both uncertain variables of the system.

Defining state variables $x_1 = \omega_r$, $x_2 = \beta$, and control input $u = \beta_1$, the state equations can be given as

$$\begin{cases} \dot{x_1} = \frac{1}{J_r + k^2 J_g}(\frac{1}{2x_1}\rho\pi R^2 v^3 C_p(\lambda, x_2) - kT_{em}) + d_1 \\ \dot{x_2} = K_d K_s(\frac{1}{K_s}u - x_2) + d_2 \end{cases} \quad (10)$$

The output expression is as follows.

$$y = x_1 \quad (11)$$

In order to gain the affine models of the wind turbine, the affine nonlinear models of single-input single-output system are formulated by Equation (12).

$$\begin{cases} \dot{x} = f(x) + g(x)u \\ y = h(x) \end{cases} \quad (12)$$

where x is the n-dimensional vector, u is the input, $f(x)$ and $g(x)$ are both smooth vector fields in $\mathbf{R}^n$, $y \in \mathbf{R}$, and $h(x)$ is a smooth nonlinear function.

Comparing Equation (12) with (10) and (11), each expression in the affine models of the wind turbine can be obtained as follows.

$$f(x) = \begin{bmatrix} f_1(x) \\ f_2(x) \end{bmatrix} = \begin{bmatrix} \frac{1}{J_r + k^2 J_g}(\frac{1}{2x_1}\rho\pi R^2 v^3 C_p(\lambda, x_2) - kT_{em}) \\ -K_d K_s x_2 \end{bmatrix} \quad (13)$$

$$g(x) = \begin{bmatrix} 0 \\ K_d K_s \end{bmatrix} \tag{14}$$

$$d^* = \begin{bmatrix} d_1 \\ d_2 \end{bmatrix} \tag{15}$$

$$h(x) = x_1 \tag{16}$$

Feedback linearization is to make input variable appear in the output expression by finding derivative of output expression. Then, an equivalent linear model of the output expression can be obtained through designing a reasonable input variable. Thereby, the procedure of feedback linearization of wind turbine model can be described as follows.

$$\begin{aligned}\dot{y} &= \frac{dh(x)}{dt} = \frac{\partial h(x)}{\partial x}\frac{\partial x}{\partial t} = \frac{\partial h(x)}{\partial x}[f(x) + g(x)u + d^*] \\ &= \frac{\partial h(x)}{\partial x}f(x) + \frac{\partial h(x)}{\partial x}g(x)u + \frac{\partial h(x)}{\partial x}d^* \end{aligned} \tag{17}$$

In accordance to Equation (16)

$$\frac{\partial h(x)}{\partial x} = [1 \quad 0] \tag{18}$$

Substituting Equations (13) and (14) into Equation (17)

$$\frac{\partial h(x)}{\partial x}f(x) = L_f h(x) = f_1(x) \tag{19}$$

$$\frac{\partial h(x)}{\partial x}g(x) = L_g h(x) = 0 \tag{20}$$

As Equation (20)=0, the input variable u will not appear in Equation (17). Thus, finding derivative of the output expression will be proceeded.

$$\begin{aligned}\ddot{y} &= \frac{\partial L_f h(x)}{\partial x}\frac{\partial x}{\partial t} = \frac{\partial L_f h(x)}{\partial x}[f(x) + g(x)u + d^*] \\ &= L_f^2 h(x) + L_g L_f h(x)u + \frac{\partial L_f h(x)}{\partial x}d^* \end{aligned} \tag{21}$$

Here

$$\begin{aligned} L_f^2 h(x) &= \frac{\partial L_f h(x)}{\partial x}f(x) = [\frac{\partial f_1(x)}{\partial x_1} \frac{\partial f_1(x)}{\partial x_2}] \begin{bmatrix} f_1(x) \\ f_2(x) \end{bmatrix} \\ &= \frac{\partial f_1(x)}{\partial x_1}f_1(x) + \frac{\partial f_1(x)}{\partial x_2}f_2(x) \end{aligned} \tag{22}$$

$$\begin{aligned} L_g L_f h(x) &= \frac{\partial L_f h(x)}{\partial x}g(x) = \begin{bmatrix} \frac{\partial f_1(x)}{\partial x_1} & \frac{\partial f_1(x)}{\partial x_2} \end{bmatrix} \begin{bmatrix} 0 \\ K_d K_s \end{bmatrix} \\ &= \frac{\partial f_1(x)}{\partial x_2}K_d K_s \end{aligned} \tag{23}$$

Therefore

$$L_g L_f h(x) \neq 0 \tag{24}$$

The input u appears in the output expression, and the relative order is equal to the order of the system. Thus, the global linearization condition can be satisfied.

Defining $d = \frac{\partial L_f h(x)}{\partial x}d^*$ and $|d| \le D$.

The error is defined as follows.

$$e = y_d - y \tag{25}$$

where y_d is the reference variable.

Thus, the sliding mode function is obtained as follows.

$$s(x, t) = \mathbf{ce} \tag{26}$$

Here

$$\mathbf{c} = [c \quad 1], \quad c > 0 \tag{27}$$

The final control law can be obtained as follows.

$$\begin{aligned} u = \frac{1}{\frac{\partial f_1(x)}{\partial x_2}K_d K_s}(v - (\frac{\partial f_1(x)}{\partial x_1}f_1(x) + \frac{\partial f_1(x)}{\partial x_2}f_2(x)) \\ + \eta sat(s)) \end{aligned} \tag{28}$$

where v is the control aid term, $\eta \ge$ D, and $sat(s)$ is the saturation function. The $sat(s)$ can be expressed by Equation (29).

$$sat(s) = \begin{cases} 1 & s > \delta \\ s/\delta & |s| \le \delta \\ -1 & s < -\delta \end{cases} \tag{29}$$

where δ is a small positive variable.

The Lyapunov function is defined by Equation (30).

$$V = \frac{1}{2}s^2 \tag{30}$$

Then

$$\begin{aligned} \dot{V} &= s\dot{s} = s(\ddot{e} + c\dot{e}) = s(\ddot{y}_d - \ddot{y} + c\dot{e}) \\ &= s(\ddot{y}_d - \frac{\partial f_1(x)}{\partial x_1}f_1(x) - \frac{\partial f_1(x)}{\partial x_2}f_2(x) \\ &\quad - \frac{\partial f_1(x)}{\partial x_2}K_d K_s u - d + c\dot{e}) \end{aligned} \tag{31}$$

Substituting the Equation (28) into Equation (31), then

$$\begin{aligned} \dot{V} &= s(\ddot{y}_d - \frac{\partial f_1(x)}{\partial x_1}f_1(x) - \frac{\partial f_1(x)}{\partial x_2}f_2(x) \\ &\quad -(v - (\frac{\partial f_1(x)}{\partial x_1}f_1(x) + \frac{\partial f_1(x)}{\partial x_2}f_2(x)) \\ &\quad + \eta sat(s)) - d + c\dot{e}) \\ &= s(\ddot{y}_d - v - \eta sat(s) - d + c\dot{e}) \end{aligned} \tag{32}$$

Defining

$$v = \ddot{y}_d + c\dot{e} \tag{33}$$

Then

$$\begin{aligned} \dot{V} &= s(-\eta sat(s) - d) = -ds - \eta\,|s| \le (D - \eta)\,|s| \le 0 \text{ or} \\ &\quad - ds - \eta\frac{|s|}{\delta} \le (D - \eta)\frac{|s|}{\delta} \le 0 \end{aligned} \tag{34}$$

The system is stable because $\dot{V}$ is negative semidefinite based on Equation (34).

When $\dot{V} \equiv 0$, according to the LaSalle invariance principle, the closed-loop system is gradually stable.

When $t \to \infty$, then $s \to 0$ and the convergence rate of s depends on η.

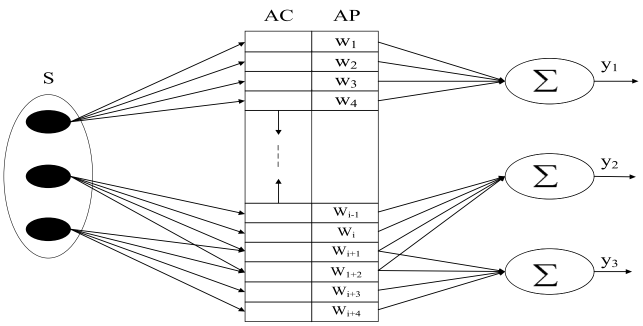

FIGURE 2. Structure diagram of CMAC.

B. NETWORK ALGORITHM FOR CEREBELLAR MODEL ARTICULATION

The CMAC is an adaptive neural network based on the table query concept [27]. The input space is divided into multiple units, each of which is allocated a specific memory address. The information in each cell is distributed to the address of the adjacent cell. The number of stored addresses is usually much smaller than the number of units that needs to handle the problem of the maximum input space. And therefore the mapping relationship is many-to-one. The contents of the table are changed by the network learning algorithm, which has multi-dimensional nonlinear mapping capability from the input to the output. As the least-mean-square algorithm is adopted, and the CMAC is a local approximation network, its learning rate is very fast. The structure diagram of the CMAC is shown in Figure 2. S is the input space, which contains the n-dimensional input vector. The inputs are mapped to the memory cells of the virtual associative memory area, AC, when they have been quantified. AP is the actual memory area.

The input space $\mathbf{u_p}$ is limited to the range $[S_{\min}, S_{\max}]$ and divided into $N + 2b$ units.

$$\mathbf{R}_p = S([\mathbf{u}_p]) = [s_1([\mathbf{u}_p]), s_2([\mathbf{u}_p]), \cdots, s_e([\mathbf{u}_p])]^T \quad (35)$$

where $[\mathbf{u_p}]$ is the quantization code and it is mapped to b units in AC.

$$\begin{cases} \omega_1 \cdots \omega_b = S_{\min} \\ \omega_i = \omega_{i-1} + \Delta\omega \quad (i = b+1, \cdots, b+N) \\ \omega_{N+b+1} \cdots \omega_{N+2b} = S_{\max} \end{cases} \quad (36)$$

where ω is the rotor speed of the wind turbine, $\Delta\omega = \frac{S_{\max}-S_{\min}}{N-1}$,

$$s_i([\mathbf{u}_p]) = \begin{cases} 1 & \mathbf{u}_p \in [\omega_i, \omega_{i+b}],\ (i = b+1, \cdots, b+N) \\ 0 \end{cases} \quad (37)$$

$$s_j([\mathbf{u}_p]) = 1, \quad j = 1, 2, \cdots b \quad (38)$$

where $s_j([\mathbf{u}_p]) = 1$ is the activated storage unit.

The c cells in AC are mapped to the actual memory, AP, using the virtual coding (compressed memory space) technique. The network output is the sum of the weights of the c cells in AP, which can be expressed as follows.

$$y_p = \sum_{j=1}^{b} w_j s_j([\mathbf{u}_p]) = R_p^T \mathbf{w}_p \quad (39)$$

where $\mathbf{w}_p = [w_1, w_2, \cdots w_j \cdots w_b]^T$, w_j is the weight value.

Then

$$y_p = \sum_{j=1}^{b} w_j = \mathbf{R}_p^T \mathbf{w}_p \quad (40)$$

The weights can be adjusted as follows.

$$\Delta w_j(t) = \gamma \frac{(u(t) - u_n(t)) s_j([\mathbf{u}_p])}{\left\| \mathbf{R}_p \right\|^2} \quad (41)$$

where γ is the learning rate of the neural network, u_t is the expected output, and $u_n(t)$ is the output of the CMAC.

Here

$$\left\| \mathbf{R}_p \right\|^2 = \sum_{j=1}^{b} s_j^2([\mathbf{u}_p]) = b \quad (42)$$

Combining the above two equations with Equation (38), the following can be obtained.

$$\Delta w_j(t) = \gamma \frac{(u_t - u_n(t))}{b} = \gamma \frac{e(t)}{b} \quad (43)$$

Gradient descent method-based the CMAC algorithm, the mean value of the errors is assigned to update the weight in each active memory cell, regardless of the different degrees of influence of the different cells. In several previous studies, the credits of the weights of all the activated memory cells were assumed to be the same, despite the different adjustment numbers in different cells. With this weight-based learning method, the memory cells that do not need to be adjusted, or that only require the minor adjustment numbers, still need to learn repeatedly. This impairs the usefulness of the network, prolongs the learning time, and reduces the learning rate. Therefore, in order to improve the learning efficiency, a method based on the credit assigned (CA) was adopted to optimize the weights in [50]. In this paper, based on [50], a balanced learning constant for the distribution of errors is introduced, and then the CA method is further improved. As a result, its convergence rate is accelerated. The adjusted values can be expressed as follows.

$$\begin{aligned} \Delta w(t) &= -\gamma \frac{\partial E(t)}{\partial w} = \gamma \frac{u(t) - u_n(t)}{b} \mathbf{R}_p \\ &= \gamma \frac{(f(j)+1)^{-\xi}}{\sum_{n=1}^{b+1} (f(j)+1)^{-\xi}} u_p(t) \mathbf{R}_p \end{aligned} \quad (44)$$

$$w(t) = w(t-1) + \Delta w(t) + \alpha(w(t) - w(t-1)) \quad (45)$$

where $f(j)$ is the updated number of the memory unit activated, ξ is the equilibrium learning constant, and ICA-CMAC is the conventional CMAC or CA-CMAC respectively when $\xi = 0$ or $\xi = 1$. That is to say that CMAC and CA-CMAC

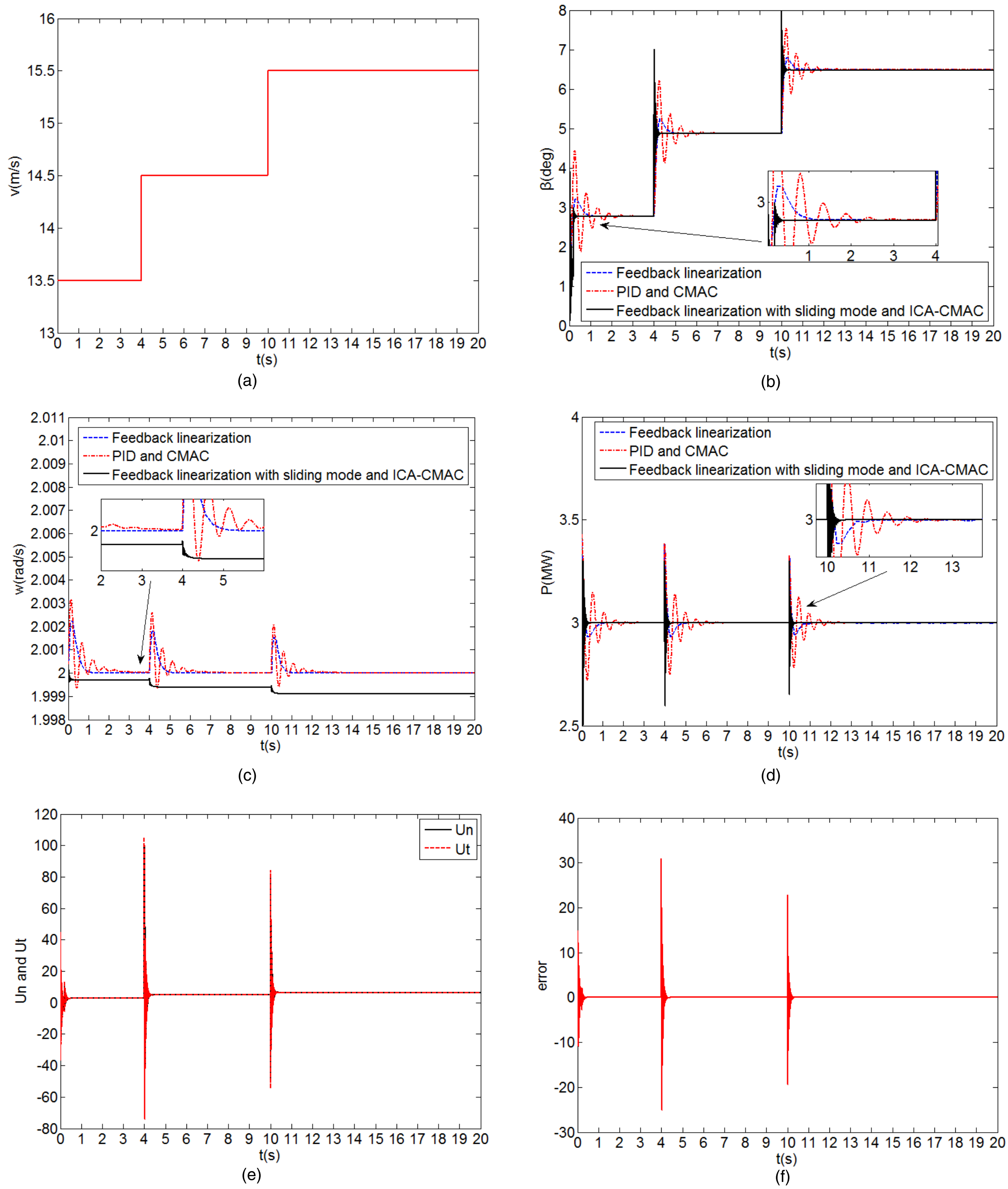

FIGURE 3. (a) Step wind speed; (b) Pitch angle under step wind speed; (c) Rotor speed under step wind speed; (d) Output power under step wind speed; (e) Comparison diagram of Un and Ut; and (f) Error between Un and Ut.

are special cases of the ICA-CMAC, while α is the inertial coefficient, $\alpha \in (0, 1)$.

In this paper, the adopted feedforward-feedback control structure has the characteristic that the control is performed by the feedback control loop at the start of the procedure. After the ICA-CMAC has learned sufficiently, it is the main factor for control in the system. Therefore, the network learning of the ICA-CMAC is strongly affected by the control performance of the feedback loop. Due to the strong nonlinear characteristics of wind turbines, the conventional PID controller that is adopted in the feedback control loop achieves low control accuracy, as a result of which the ICA-CMAC

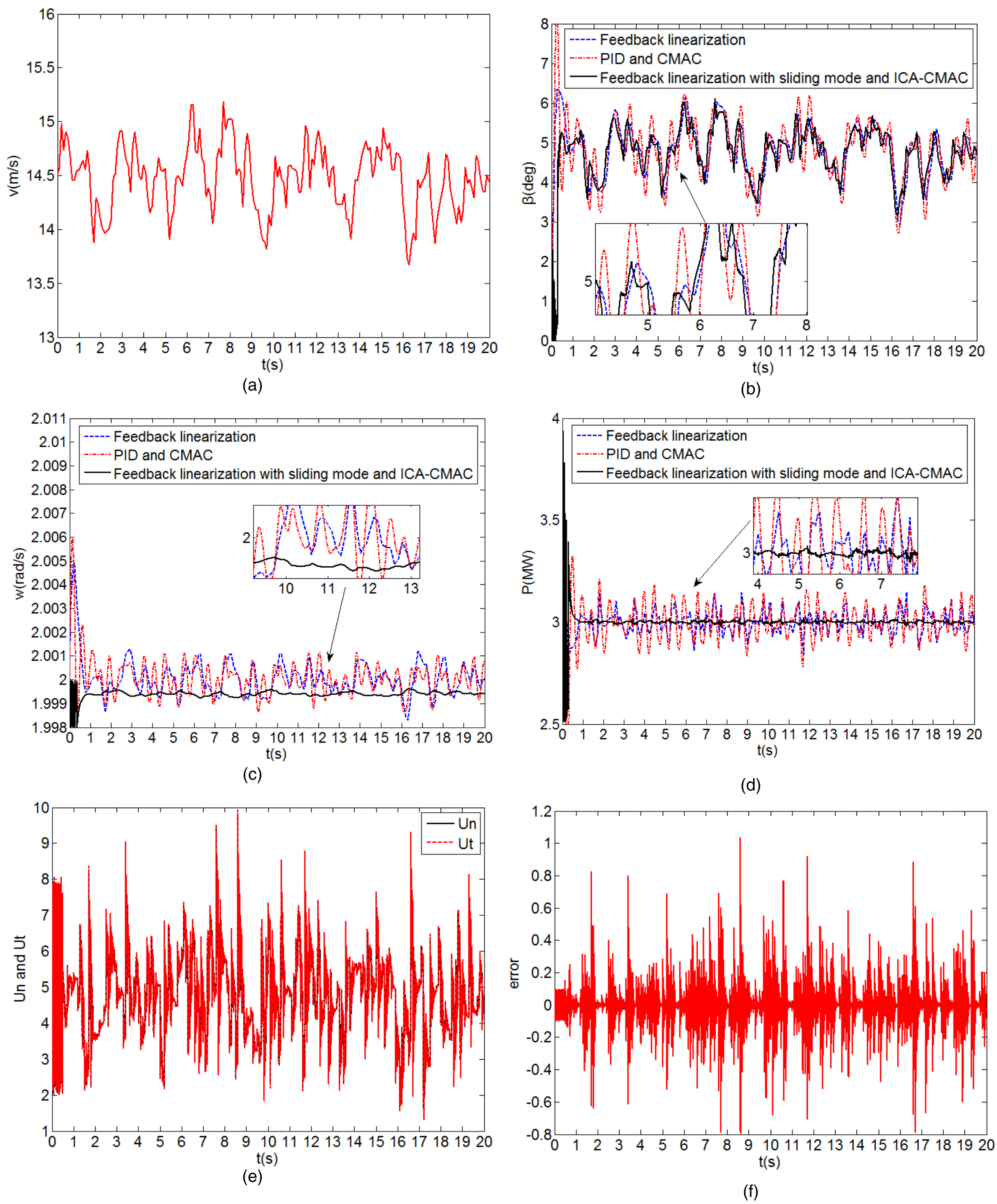

FIGURE 4. (a) Random wind speed; (b) Pitch angle under random wind speed; (c) Rotor speed under random wind speed; (d) Output power under random wind speed; (e) Comparison diagram of Un and Ut; (f) Error between Un and Ut.

learning results are not ideal. In order to overcome the nonlinearity of the wind turbine and improve the accuracy of the inner loop feedback control, the control law is designed by the feedback linearization method, which is a powerful tool to solve nonlinear problems. Rigorous mathematical derivation is employed and input state appears in the output equation. Then, the appropriate control law can be designed to obtain the linear output expression. However, the robustness of the system cannot be guaranteed when the feedback linearization method is adopted. On the other hand, the sliding mode variable structure control has a switching characteristic. And furthermore its system structure changes with time. This control characteristic can force the system to move up and down along a specified state trajectory under certain conditions,

TABLE 1. Parameters of the wind turbine.

Symbol	Parameter	Value
P_{rated}	Rated output power	3000KW
V_{rated}	Rated wind speed	12m/s
R	Radius of the rotor	47.5m
J_r	Inertia moment of the rotor	6250000kg·m^2
J_g	Inertia moment of the generator	15kg·m^2
k	Drive ratio	80
r_1	Stator winding resistance	0.0148Ω
r_2	Rotor winding resistance calculated to stator	0.0370Ω
$x_{1\sigma}$	Leakage reactance	0.0727Ω
$x_{2\sigma}$	Leakage calculated to stator side	0.0863Ω
x_m	Excitation reactance	2.0000Ω

TABLE 2. Parameters of the proposeed controller.

Symbol	Parameter	Value
c	Design parameter of the sliding mode function	10
η	Sliding mode switching gain	3
δ	Boundary Parameter of saturation function	0.05
b	Generalization parameter of the ICA-CMAC network	5
ξ	Equilibrium learning constant	0.7
α	Inertia value	0.04
γ	Learning rate of the ICA-CMAC network	0.1

which is called the sliding mode. This sliding mode algorithm can be designed but will be unaffected by the parameters and perturbations of the system. Therefore, a system controlled by the sliding mode has strong robustness. Furthermore, the sliding mode control is combined with the feedback linearization method to improve both system performance and the accuracy of the inner loop feedback control, which is used as a learning object for the ICA-CMAC.

IV. SIMULATION AND RESULTS ANALYSIS

In order to verify the effectiveness of the proposed algorithm, a specific type of wind turbine is adopted as the control object. The parameters of the wind turbine are expressed in TABLE 1. The parameters of the proposed controller are shown in TABLE 2.

Checking step response is an effective way to verify the performance of the controller. Therefore, the response speed, overshoot and steady-state performance of the pitch system are verified by the step wind speed. At the start of the simulation, since the ICA-CMAC has not achieved learning procedure from closed-loop control, the control performance is not yet satisfactory. After a period of learning, the ICA-CMAC plays the major role in the control system.

Figure 3b, Figure 3c and Figure 3d show that when a feedback linearization controller, a PID or a CMAC controller is used, the system has a large overshoot, and the adjusting time is long. Furthermore, from the comparison of the feedback linearization controller with the PID and CMAC controller, it is found that the overshoot of feedback linearization is smaller than that of PID and CMAC. In addition, as the CMAC firstly needs to learn PID controller, its adjusting time is longer than that of the feedback linearization controller at the start of the simulation. Therefore, considering the relative advantages of the two control algorithms, feedback linearization is used to design the feedback controller and sliding mode algorithm is adopted to optimize its performance. At the same time, the improved CMAC, ICA-CMAC, is used to design the feedforward controller. Thus, using the proposed compound controller, the system quickly responds in respect to the wind speed, with a very small steady-state error. As the pitch angle can be adjusted very accurately, the output power of the wind turbine can also be well maintained at the rated value. The power output shown in Figure 3(d) verifies this conclusion.

In practice, step wind speed is extremely rare. In most cases, the wind speed is random. Therefore, in order to further verify the practicality of the proposed controller, the output power is controlled under random wind speed as shown in Figure 4b, Figure 4c and Figure 4d. These show that when the compound controller proposed in this paper is used, the output power can be well maintained at the rated value, and the fluctuation is smaller than those of the other controllers. Thus, the desired control targets can be fulfilled.

V. CONCLUSION

As a wind turbine is a strongly nonlinear system with large hysteresis, it is difficult to achieve satisfactory control with conventional controllers. In order to realize effective control for a wind turbine, a compound feedforward-feedback control is developed here. In the feedback control loop, feedback linearization in combination with sliding mode theory is adopted, both to achieve stable control and improve the robustness. In the feedforward loop, the ICA-CMAC controller is used. This controller not only approximates the nonlinear model well but also applies a control quantity to the system ahead of time to compensate for the delay caused by the large inertia of the pitch system.

The compound control method adopted in this paper not only keep the output power at the rated value but can also has a fast response speed, short adjusting time and small steady-state error under random wind speed. And the desired control targets can be achieved.

REFERENCES

[1] C.-S. Wang and M.-H. Chiang, "A novel dynamic co-simulation analysis for overall closed loop operation control of a large wind turbine," *Energies*, vol. 9, no. 8, pp. 637–656, Aug. 2016.

[2] X. Jin, Y. Wang, W. Ju, J. He, and S. Xie, "Investigation into parameter influence of upstream deflector on vertical axis wind turbines output power via three-dimensional CFD simulation," *Renew. Energy*, vol. 115, pp. 41–53, Jan. 2018.

[3] S. T. Kandukuri, A. Klausen, H. R. Karimi, and K. G. Robbersmyr, "A review of diagnostics and prognostics of low-speed machinery towards wind turbine farm-level health management," *Renew. Sustain. Energy Rev.*, vol. 53, pp. 697–708, Jan. 2016.

[4] K.-Y. Oh, J.-Y. Park, J.-S. Lee, and J. Lee, "Implementation of a torque and a collective pitch controller in a wind turbine simulator to characterize the dynamics at three control regions," *Renew. Energ.*, vol. 79, pp. 150–160, Jul. 2015.

[5] J. Dang, J. Seuss, L. Suneja, and R. G. Harley, "SOC feedback control for wind and ESS hybrid power system frequency regulation," *IEEE J. Emerg. Sel. Topics Power Electron.*, vol. 2, no. 1, pp. 79–86, Mar. 2014.

[6] T. Bakka and H. R. Karimi, "Bond graph modeling and simulation of wind turbine systems," *J. Mech. Sci. Technol.*, vol. 27, no. 6, pp. 1843–1852, Jun. 2013.

[7] X. Jin, L. Li, W. Ju, Z. Zhang, and X. Yang, "Multibody modeling of varying complexity for dynamic analysis of large-scale wind turbines," *Renew. Energy*, vol. 90, pp. 336–351, May 2016.

[8] T.-P. Chang, F.-J. Liu, H.-H. Ko, S.-P. Cheng, L.-C. Sun, and S.-C. Kuo, "Comparative analysis on power curve models of wind turbine generator in estimating capacity factor," *Energy*, vol. 73, pp. 88–95, Aug. 2014.

[9] T. Bakka and H. R. Karimi, "Robust H_∞ dynamic output feedback control synthesis with pole placement constraints for offshore wind turbine systems," *Math. Problems Eng.*, vol. 2012, pp. 1–18, Sep. 2012.

[10] H. Li, C. Yang, Y. Hu, X. Liao, Z. Zeng, and C. Zhe, "An improved reduced-order model of an electric pitch drive system for wind turbine control system design and simulation," *Renew. Energ.*, vol. 93, pp. 188–200, Aug. 2016.

[11] M. Q. Duong, F. Grimaccia, S. Leva, M. Mussetta, and E. Ogliari, "Pitch angle control using hybrid controller for all operating regions of SCIG wind turbine system," *Renew. Energy*, vol. 70, pp. 197–203, Oct. 2014.

[12] F. Dunne, L. Y. Pao, A. D. Wright, B. Jonkman, and N. Kelley, "Adding feedforward blade pitch control to standard feedback controllers for load mitigation in wind turbines," *Mechatronics*, vol. 21, no. 4, pp. 682–690, Jun. 2011.

[13] C.-M. Sung and M.-C. Han, "Design and performance evaluation of hinge type pitch control system in small-size wind turbine," *Int. J. Precision Eng. Manuf. Green Technol.*, vol. 3, no. 4, pp. 335–341, Oct. 2016.

[14] H. Jafarnejadsani, J. Pieper, and J. Ehlers, "Adaptive control of a variable-speed variable-pitch wind turbine using radial-basis function neural network," *IEEE Trans. Control Syst. Technol.*, vol. 21, no. 6, pp. 2264–2272, Nov. 2013.

[15] B. Han, L. Zhou, F. Yang, and Z. Xiang, "Individual pitch controller based on fuzzy logic control for wind turbine load mitigation," *IET Renew. Power Generat.*, vol. 10, no. 5, pp. 687–693, May 2016.

[16] T. L. Van, T. H. Nguyen, and D. C. Lee, "Advanced pitch angle control based on fuzzy logic for variable-speed wind turbine systems," *IEEE Trans. Energy Convers.*, vol. 30, no. 2, pp. 578–587, Jun. 2015.

[17] A. Díaz de Corcuera, A. Pujana-Arrese, J. M. Ezquerra, A. Milo, and J. Landaluze, "Linear models-based LPV modelling and control for wind turbines," *Wind Energy*, vol. 18, no. 7, pp. 1151–1168, Jul. 2015.

[18] Z. Civelek, E. Çam, M. Lüy, and H. Mamur, "Proportional-integral-derivative parameter optimisation of blade pitch controller in wind turbines by a new intelligent genetic algorithm," *IET Renew. Power Generat.*, vol. 10, no. 8, pp. 1220–1228, Sep. 2016.

[19] M. Zhu, J. Liu, Z. Lin, and H. Meng, "Mixed H_2/H_∞ pitch control of wind turbine generator system based on global exact linearization and regional pole placement," *Int. J. Mach. Learn. Cybern.*, vol. 7, no. 5, pp. 921–930, Oct. 2016.

[20] M. L. Corradini, G. Ippoliti, and G. Orlando, "An observer-based blade-pitch controller of wind turbines in high wind speeds," *Control Eng. Pract.*, vol. 58, pp. 186–192, Jan. 2017.

[21] A. Lasheen and A. L. Elshafei, "Wind-turbine collective-pitch control via a fuzzy predictive algorithm," *Renew. Energy*, vol. 87, pp. 298–306, Mar. 2016.

[22] A. S. Yilmaz and Z. Özer, "Pitch angle control in wind turbines above the rated wind speed by multi-layer perceptron and radial basis function neural networks," *Expert Syst. Appl.*, vol. 36, no. 6, pp. 9767–9775, Aug. 2009.

[23] Y. Xiao, Y. Hong, X. Chen, and W. Huo, "Switching control of wind turbine sub-controllers based on an active disturbance rejection technique," *Energies*, vol. 9, no. 10, pp. 793–811, Oct. 2016.

[24] P. Bagheri and Q. Sun, "Adaptive robust control of a class of non-affine variable-speed variable-pitch wind turbines with unmodeled dynamics," *ISA Trans.*, vol. 63, pp. 233–241, Jul. 2016.

[25] D. Li, Y. Song, W. Cai, P. Li, and H. R. Karimi, "Wind turbine pitch control and load mitigation using an L_1 adaptive approach," *Math. Problems Eng.*, vol. 2014, pp. 1–11, Apr. 2014.

[26] Z. Yunqian, C. Zhe, and C. Ming, "Proportional resonant individual pitch control for mitigation of wind turbines loads," *IET Renew. Power Generat.*, vol. 7, no. 3, pp. 191–200, May 2013.

[27] D. Chen, P. Xu, R. Zhou, and X. Ma, "A CMAC-PID based on pitch angle controller for direct drive permanent magnet synchronous wind turbine," *J. Vibrat. Control*, vol. 22, no. 6, pp. 1657–1666, Apr. 2016.

[28] C.-S. Wang and M.-H. Chiang, "A novel pitch control system of a large wind turbine using two-degree-of-freedom motion control with feedback linearization control," *Energies*, vol. 9, no. 10, pp. 791–808, Oct. 2016.

[29] N. Wang, J.-C. Sun, M. Han, Z. Zheng, and M. J. Er, "Adaptive approximation-based regulation control for a class of uncertain nonlinear systems without feedback linearizability," *IEEE Trans. Neural Netw. Learn. Syst.*, to be published.

[30] T. Bakka, H. R. Karimi, and S. Christiansen, "Linear parameter-varying modelling and control of an offshore wind turbine with constrained information," *IET Control Theory Appl.*, vol. 8, no. 1, pp. 22–29, Jan. 2014.

[31] Y. Wang, Y. Xia, H. Shen, and P. Zhou, "SMC design for robust stabilization of nonlinear Markovian jump singular systems," *IEEE Trans. Autom. Control*, vol. 63, no. 1, pp. 219–224, Jan. 2018.

[32] N. Wang, J.-C. Sun, and M. J. Er, "Tracking-error-based universal adaptive fuzzy control for output tracking of nonlinear systems with completely unknown dynamics," *IEEE Trans. Fuzzy Syst.*, to be published.

[33] Y. Si, H. R. Karimi, and H. Gao, "Modelling and optimization of a passive structural control design for a spar-type floating wind turbine," *Eng. Struct.*, vol. 69, pp. 168–182, Jun. 2014.

[34] C. Evangelista, P. Puleston, F. Valenciaga, and L. M. Fridman, "Lyapunov-designed super-twisting sliding mode control for wind energy conversion optimization," *IEEE Trans. Ind. Electron.*, vol. 60, no. 2, pp. 538–545, Feb. 2013.

[35] Y. Wang, H. Shen, H. R. Karimi, and D. Duan, "Dissipativity-based fuzzy integral sliding mode control of continuous-time T-S fuzzy systems," *IEEE Trans. Fuzzy Syst.*, to be published.

[36] S. Ding, A. Levant, and S. Li, "Simple homogeneous sliding-mode controller," *Automatica*, vol. 67, pp. 22–32, May 2016.

[37] F. Valenciaga and P. F. Puleston, "High-order sliding control for a wind energy conversion system based on a permanent magnet synchronous generator," *IEEE Trans. Energy Convers.*, vol. 23, no. 3, pp. 860–867, Sep. 2008.

[38] C. A. Evangelista, A. Pisano, P. Puleston, and E. Usai, "Receding horizon adaptive second-order sliding mode control for doubly-fed induction generator based wind turbine," *IEEE Trans. Control Syst. Technol.*, vol. 25, no. 1, pp. 73–84, Jan. 2017.

[39] S. M. Mozayan, M. Saad, H. Vahedi, H. Fortin-Blanchette, and M. Soltani, "Sliding mode control of PMSG wind turbine based on enhanced exponential reaching law," *IEEE Trans. Ind. Electron.*, vol. 63, no. 10, pp. 6148–6159, Oct. 2016.

[40] N. Wang, S. Lv, W. Zhang, Z. Liu, and M. J. Er, "Finite-time observer based accurate tracking control of a marine vehicle with complex unknowns," *Ocean Eng.*, vol. 145, pp. 406–415, Nov. 2017.

[41] S. Ding and S. Li, "Second-order sliding mode controller design subject to mismatched term," *Automatica*, vol. 77, pp. 388–392, Mar. 2017.

[42] H. R. Karimi, N. A. Duffie, and S. Dashkovskiy, "Local capacity H_∞ control for production networks of autonomous work systems with time-varying delays," *IEEE Trans. Autom. Sci. Eng.*, vol. 7, no. 4, pp. 849–857, Oct. 2010.

[43] H. R. Karimi and H. Gao, "Mixed H_2/H_∞ output-feedback control of second-order neutral systems with time-varying state and input delays," *ISA Trans.*, vol. 47, no. 3, pp. 311–324, 2008.

[44] Y. Yuan and J. Tang, "Adaptive pitch control of wind turbine for load mitigation under structural uncertainties," *Renew. Energy*, vol. 105, pp. 483–494, May 2017.

[45] M.-H. Chiang, "A novel pitch control system for a wind turbine driven by a variable-speed pump-controlled hydraulic servo system," *Mechatronics*, vol. 21, no. 4, pp. 753–761, Jun. 2011.

[46] X. Yang, J. Li, and W. Liu, "Petri net model and reliability evaluation for wind turbine hydraulic variable pitch systems," *Energies*, vol. 4, no. 6, pp. 978–997, Jun. 2011.

[47] N. Wang, S.-F. Su, J. Yin, Z. Zheng, and M. J. Er, "Global asymptotic model-free trajectory-independent tracking control of an uncertain marine vehicle: An adaptive universe-based fuzzy control approach," *IEEE Trans. Fuzzy Syst.*, to be published.
[48] R. Sakthivel, H. R. Karimi, M. Joby, and S. Santra, "Resilient sampled-data control for Markovian jump systems with an adaptive fault-tolerant mechanism," *IEEE Trans. Circuits Syst. II, Exp. Breifs*, vol. 64, no. 11, pp. 1312–1316, Nov. 2017.
[49] Y. Wei, J. Qiu, and H. R. Karimi, "Reliable output feedback control of discrete-time fuzzy affine systems with actuator faults," *IEEE Trans. Circuits Syst. I, Reg. Papers*, vol. 64, no. 1, pp. 170–181, Jan. 2017.
[50] S.-F. Su, T. Tao, and T.-H. Hung, "Credit assigned CMAC and its application to online learning robust controllers," *IEEE Trans. Syst., Man, Cybern. B, Cybern.*, vol. 33, no. 2, pp. 202–213, Apr. 2003.

HAIJUN REN received the Ph.D. degree in mechanical engineering from Chongqing University, Chongqing, China, in 2011.

From 2011 to 2014, he was a Lecturer with the School of Automation, Chongqing University of Posts and Telecommunications, Chongqing, China. In 2015, he was an Associate Professor with the School of Advanced Manufacture and Engineering, Chongqing University of Posts and Telecommunications, Chongqing, China. From 2015 to 2016, he was a Visiting Scholar with Institute of Industrial Science, The University of Tokyo.

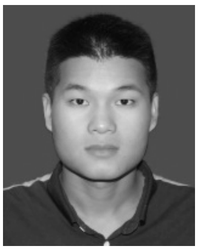

HAO ZHANG received the B.E. degree in mechanical engineering from the Taiyuan University of Science and Technology, Taiyuan, China, in 2016.

He is currently pursuing the M.S. degree with the School of Advanced Manufacture and Engineering, Chongqing University of Posts and Telecommunications, Chongqing, China.

HUANHUI ZHOU received the B.E. degree in electronic and information engineering from the Chongqing University of Technology, Chongqing, China, in 2014.

He is currently pursuing the M.S. degree with the School of Advanced Manufacture and Engineering, Chongqing University of Posts and Telecommunications, Chongqing, China.

PING ZHANG received the B.E. degree in electronic and information engineering from Nanyang Normal University, Nanyang, China, in 2015.

She is currently pursuing the M.S. degree with the School of Advanced Manufacture and Engineering, Chongqing University of Posts and Telecommunications, Chongqing, China.

XIN LEI received the B.E. degree in electronic and information engineering from Wuhan Textile University, Wuhan, China, in 2015.

He is currently pursuing the M.S. degree with the School of Advanced Manufacture and Engineering, Chongqing University of Posts and Telecommunications, Chongqing, China.

GUANG DENG received the B.E. degree in mechanical engineering from the North China Institute of Aerospace Engineering, Langfang, China, in 2017.

He is currently pursuing the M.S. degree with the School of Advanced Manufacture and Engineering, Chongqing University of Posts and Telecommunications, Chongqing, China.

BIN HOU received the B.E. degree in mechanical engineering from the Tianjin University of Technology, China, in 2017. He is currently pursuing the M.S. degree with the School of Advanced Manufacture and Engineering, Chongqing University of Posts and Telecommunications, Chongqing, China.